Wave propagation and nonequilibrium interphase processes in transient two-phase flows

D. Assimacopoulos*

Computational Fluid Dynamics Unit, Imperial College, London, UK
(Received December 1986; revised October 1987)

A transient, one-dimensional, compressible, two-phase flow is studied. Two different flow regimes, dispersed and stratified, as well as momentum, heat, and mass-interphase processes are considered. Numerical solutions and calculation of wave speeds are shown for different flow conditions. Simple tests using analytical solutions for approximate flow conditions are introduced. Computational results are compared and found to be in excellent agreement.

Keywords: two-phase flow, compressible flow, wave propagation

Introduction

The problem considered

The present study is concerned with a transient, one-dimensional, compressible, two-phase flow in a confined duct. The momentum, heat, and mass-interphase processes of two different flow regimes, one dispersed and one gravity-stratified, are considered.

Practical relevance

Two-phase transients can be found in many industrial pipeline flows. Typical examples of such situations are (a) two-phase flow in petroleum lines, (b) the presence of free gas in sewage lines, (c) the discharge of primary coolant in a pressurised water reactor following a pipe rupture, (d) the release of air and other gases as a result of a sudden pressure reduction, and (e) the release of a gas during liquid-column separation.[1]

Previous work

The various flow regimes which are present in two-phase flows, the slip velocity between the phases, nonequilibrium effects of subcooling or superheating as well as the strong coupling of the thermal and hydrodynamic flow fields give rise to complex and, therefore, difficult-to-analyse flow patterns. It is well known, for example, that small amounts of free gas in a liquid can dramatically reduce the velocity of sound in the medium.[2] An important way to verify and quantify some of the nonsteady aspects of two-phase interactions is the prediction of wave propagation phenomena. Ability to predict the wave speed in two-phase flows has importance in such diverse areas as the onset of slug flow,[3-4] the relation between choked flow and sonic velocity,[5-6] the formation of shock waves,[7-8] or the determination of mechanical impulse loads and blowdown starting transients.

If the disturbances are not very strong, wave velocities and attenuation of wavefronts can be calculated on the basis of a linearisation of the governing flow equations and on consideration of the eigenvalues of the resulting dispersion equation. Interesting results have been obtained by Mecredy and Hamilton,[9] Ardron and Duffey,[10] and Cheng *et al.*[11] Using the same approach, we can also explore stability problems concerning particular mathematical models. Although stability analysis using the linearised form of a strong nonlinear system cannot always provide reliable results, it can offer enhanced possibilities in the modelling of two-phase flows, as, in this case, Stuhmiller,[12] Ardron,[13] Wallis and Hutchings,[14] and Jones and Prosperetti[15] have shown.

* Present address: Department of Chemical Engineering, National Technical University of Athens, Greece

When strong disturbances need to be considered, the above-mentioned analytical approach cannot be applied, and numerical solutions are inevitable. Wave propagation in unsteady, incompressible, two-phase flows has been studied numerically by using the IPSA algorithm,[16] and results have been reported along with comparisons to analytical solutions by Baghdadi *et al.*[17] and Kurosaki and Spalding.[18] Some preliminary results for a compressible flow have been presented by Spalding.[19] Hancox *et al.*[20] have also performed some calculations for a compressible stratified mixture using an explicit numerical scheme.

Objectives of the present work

In the present work a two-fluid model is used which explicitly allows for momentum, mass, and heat transfer at the interface. For the calculations performed and reported here, the IPSA algorithm has been used. The objectives of the work are to

a. introduce simple approximating analytical solutions so that the accuracy of the computational results can be tested
b. demonstrate that compressible two-phase flows with nonequilibrium interphase processes and pressure or gravity waves can be accurately simulated at different flow regimes
c. suggest that simulation of that sort can be used to investigate the effects of the interphase correlations leading to a better understanding of the underlying physical mechanisms

Description of the process simulated

The process we are to model concerns the transient two-phase flow in a duct and, in particular, the propagation of a wavefront developed because of the compressibility effects appearing in the light phase. The duct has a length of 10 m, a rectangular cross section, and both ends closed. The duct walls are considered adiabatic. Both fluids initially have uniform pressures and uniform velocities.

Two different flow systems are studied. The first is a two-phase system for which only interphase momentum transfer is allowed. The two phases are assumed to be air and water of densities 1 kg/m^3 and 1000 kg/m^3, respectively, and equal temperatures. In the second system a two-phase flow of steam and water is considered. In addition to momentum, interphase heat and mass transfer processes are active. The system initially is at a condition of thermodynamic equilibrium under atmospheric pressure and a temperature of 100°C. The densities of the vapour and liquid phase are 0.596 kg/m^3 and 960.61 kg/m^3, respectively. The latent heat of vaporisation is 2257 kJ/kg.

In both cases the light fluid is assumed to be compressible, and the heavy fluid incompressible. Each fluid experiences friction with the other phase because of unequal phase velocities, but no wall friction is assumed because its influence on the sonic velocity is not very significant.[9] Two classes of flow will be studied: (a) a dispersed flow in which it is assumed that no gravitational forces act, and (b) a stratified flow in which gravity acts normally to the main flow direction but the stratification of the fluids produces a resultant force parallel to the flow direction.

The system is set in motion because of the initially uniform and equal fluid velocities. As the two fluids approach the upstream closed end of the duct they retard with a consequent compression of the light phase. The increase in pressure results in a pressure wave being propagated upstream and conveying the retardation of flow to the column of fluid approaching the closed end along the upstream pipeline. There are two links between the fluids, the first coming from the volume compatibility condition, the second from the interphase transport mechanisms. Thus, the pressure wave travels through the fluid at the appropriate sonic velocity, which depends not only on the properties of the medium but also on the interphase transfer processes. Similarly, on the downstream side of the pipe the retardation of flow causes a pressure reduction, resulting in a negative pressure wave which propagates along the downstream pipe and, in its turn, retards the fluid flow.

The passage of the pressure wave along the pipe is accompanied by a thermal wave propagating with the same velocity. Temperature variations along the pipe result in small vaporisations and condensations at the interfaces involved. If thermodynamic equilibrium is to be maintained, the heat transfer should be rapid enough. Otherwise the process of condensation-vaporisation cannot follow the wave propagation, and when there is no heat transfer at all the sonic velocity finds an upper limit.[7]

Finally, when a stratified flow exists, a gravity wave also is expected to propagate along the pipe with a velocity much slower than that of the pressure wave.

From the above discussion it is obvious that for the flow considered there are three classes of physical phenomena, each one having a different characteristic time scale of evolution. These are interphase exchanges, fluid convection, and wave propagation. It is therefore necessary that the model which will simulate the flow under consideration as well as the numerical algorithm which will solve the equations be able to predict well all the phenomena discussed.

Mathematical formulation

The two-fluid model of gas-liquid flow incorporates six separate conservation equations for the flow of the gas and liquid phases. These are derived from a balance of fluxes over a control volume large enough compared with microscopic length scales (e.g., bubble radius) but small relative to wavelength. The time scale should also be large compared with microscale fluctuations (e.g., turbulence) but small with respect to macroscopic scales of interest (e.g., wave propagation period and interphase transport processes). Further it is assumed that each phase is a continuum, so derivatives can uniquely be defined, the density of the liquid phase

is constant, and viscous effects other than interphase friction and conduction effects within phases are negligible.

The following dependent variables are used:

- velocities of gas and liquid: u_g, u_ℓ
- pressure: P (in stratified flow a gravity source term G is active for the liquid phase)
- stagnation enthalpies of gas and liquid: h_g, h_ℓ
- volume fractions of gas and liquid: r_g, r_ℓ
- density of gas: ρ_g

The independent variables are the distance measured along the duct, x, and the time t. The equations have the following form:

Continuity.

$$\frac{\partial(r_g\rho_g)}{\partial t} + \frac{\partial(r_g\rho_g u_g)}{\partial x} = \dot{m}_{\ell g} \tag{1}$$

$$\frac{\rho_\ell \partial(r_\ell)}{\partial t} + \frac{\rho_\ell \partial(r_\ell u_\ell)}{\partial x} = -\dot{m}_{\ell g} \tag{2}$$

Momentum.

$$\frac{\partial(r_g\rho_g u_g)}{\partial t} + \frac{\partial(r_g\rho_g u_g^2)}{\partial x} = -r_g\frac{\partial P}{\partial x} + F_d + \dot{m}_{g\ell}u_\ell \tag{3}$$

$$\rho_\ell\frac{\partial(r_\ell u_\ell)}{\partial t} + \rho_l\frac{\partial(r_\ell u_\ell^2)}{\partial x} = -r_\ell\frac{\partial P}{\partial x} - F_d - \dot{m}_{\ell g}u_g + G \tag{4}$$

Enthalpy.

$$\frac{\partial[r_g\rho_g(h_g - P/\rho_g)]}{\partial t} + \frac{\partial(r_g\rho_g u_g h_g)}{\partial x} = u_\ell F_d + \dot{Q}_g + \dot{m}_{\ell g}(h_{gi} - h_g) \tag{5}$$

$$\frac{\partial[r_\ell\rho_\ell(h_\ell - P/\rho_\ell)]}{\partial t} + \frac{\partial(r_\ell\rho_\ell u_\ell h_\ell)}{\partial x} = -u_g F_d - \dot{Q}_\ell - \dot{m}_{\ell g}(h_{\ell i} - h_\ell) \tag{6}$$

Finally, the volume fractions are related by the compatibility equation

$$r_g + r_\ell = 1 \tag{7}$$

In order to integrate the conservation equations, the conditions at the interface should be defined, and additional relations expressing the interphase transfer processes in terms of the bulk phase properties should be implemented. As far as the interface conditions are concerned, it is assumed that interface pressures are equal to the common phase pressure (for stratified flow a gravity term is active in the liquid momentum balance) and that the enthalpy values at the interface are constant and equal to their initial saturation values.

Three kinds of interphase source terms are present in the equations above: those connected to interphase drag force F_d, those connected with the interphase mass transfer rate $\dot{m}_{\ell g}$, and those connected with the heat transfer from one phase to the other, $\dot{Q}_g$ and $\dot{Q}_\ell$. Finally, the gravity source term G introduces a second pressure for the stratified flow.

The interphase drag force is modelled by

$$F_d = f(u_\ell - u_g)$$

where the interphase drag coefficient obeys the linear law

$$f = c_d\rho_g r_g r_\ell$$

The interphase mass transfer contributes to the momentum of each phase a quantity equal to the mass transfer rate times the velocity of the mass. The interphase mass transfer rate is calculated by using a heat balance over a control volume just enclosing the interface. This gives

$$\dot{m}_{\ell g} = \frac{k_{gi}(h_g - h_{gi}) + k_{\ell i}(h_\ell - h_{\ell i})}{h_{gi} - h_{\ell i}}$$

where the subscript i denotes values at the interface (saturation values) and k_{gi}, $k_{\ell i}$ are heat transfer coefficients from the bulk of the gas phase to interface and from the bulk of the liquid phase to interface, respectively. It is assumed that these coefficients also obey a linear law:

$$k_{gi} = k_g\rho_g r_g r_\ell \quad \text{and} \quad k_{\ell i} = k_\ell\rho_\ell r_g r_\ell$$

The interphase heat transfer terms are equal to

$$\dot{Q}_\ell = k_{\ell i}(h_\ell - h_{\ell i}) \quad \text{and} \quad \dot{Q}_g = k_{gi}(h_g - h_{gi})$$

The gravity source term is active only when a stratified flow is considered, and it is given by

$$G = A_g(\rho_\ell - \rho_g)r_\ell\frac{\partial r_\ell}{\partial x}$$

where A is a constant.

Density is assumed to be related to pressure by an ideal-gas law equation of state. Hence

$$\rho_g = P/RT$$

Since the energy equations (5) and (6) are written for the enthalpy variables, an additional relationship between enthalpy and temperature is needed. Curve fitting of the temperature-enthalpy relationship based on the ideal-gas heat capacity data from 0° to 150°C gives the linear equation

$$T = -1115.6 + 5.29\cdot10^{-4}h_g$$

We shall close this section with a remark on the mathematical difficulties that the system of equations (1)–(6) can pose when no interphase transfer processes and no second pressure for the liquid phase are present. Writing the system in the form $\partial_t u + A\partial_x u = 0$, it can be shown[21] that the matrix A has a pair of complex eigenvalues. For a linear system, this means that the solutions may not depend continuously on the initial conditions. This argument has not been proven to apply to nonlinear systems, but even were it so the situation would not be hopeless since the inclusion of any nonzero viscosity makes the model well-posed.[21] Since

the inevitable numerical diffusion introduces artificial viscosity during the numerical solution of the equations, the argument remains purely a theoretical one.

Finite-domain equations and solution procedure

The finite-domain equations are derived by integrating the governing differential equations over the volume of a cell enclosing a grid node. A staggered grid was used, and therefore the control volume for continuity is different from that for momentum. For volume fractions and enthalpies these control volumes are those centered on the grid nodes. The control volumes for the velocities are displaced in the x-direction by a distance which places the relevant velocity locations at the mid-distance of two consecutive grid nodes. The result of the integration is expressed in terms of the values of the variables pertaining to grid nodes. This is done by way of interpolation assumptions and leads to a set of equations which, because of their high degree of non-linearity and interlinkage, are solved by an iteration method of a successive-adjustment nature. The procedure used for the numerical studies of the present work is the IPSA algorithm of Spalding[16,19,22] and the PHOENICS computer code,[23] which embodies this.

Grid- and time-independency tests have been carried out on the basis of the wave velocity discussed in the subsequent section on wave velocity. Computational cells of 0.1 m and time steps of 2.10^{-4} s for the pressure wave studies and 0.05 s for the gravity wave studies were employed. The CPU time taken was $8.5 \cdot 10^{-4}$ s per grid node/per sweep/per time-step/per main variable on a Perkin-Elmer 3220 minicomputer.

Presentation of results

For all flow simulations to be discussed presently, SI units have been used, and unless otherwise specified the following initial conditions have been assumed:

$$u_{g0} = u_{\ell 0} = -4.0\,\text{m/s}$$
$$P_{g0} = 1.10^5\,\text{Pa}$$
$$r_\ell = 0.01$$

where the subscript 0 refers to the initial conditions. Also, all the profiles are plotted for half the length of the duct.

Isothermal flow of an air-water system

The thermodynamic evolution of the compressible fluid was assumed to be known and obeying an isentropic law. There was no need, therefore, for solving the enthalpy equations, and the pressure was related to gas density by

$$\rho_g = \alpha P^{1/\gamma}$$

where α is a constant defined by the initial conditions and γ is the specific heat ratio, equal to 1.4 for air. Simulations were performed for dispersed and stratified flows. Different values of the interphase friction were considered, varying progressively from a frictionless flow to a homogeneous equilibrium model (HEM).

Dispersed flow. As expected, a wave is formed for each dependent variable of the compressible fluid (*Figures 1,2,3*). For small values of the interphase friction no disturbance is shown to propagate in the liquid. Because of its initial velocity the incompressible fluid is moving and fills the upstream end of the duct. It is only when the friction increases greatly that the liquid starts to follow the motion of the gas (*Figure 4*). As friction increases, the velocity of the pressure wave decreases, and since momentum is transferred from liquid to gas, the pressure rise of the gas increases (*Figures 2,3*).

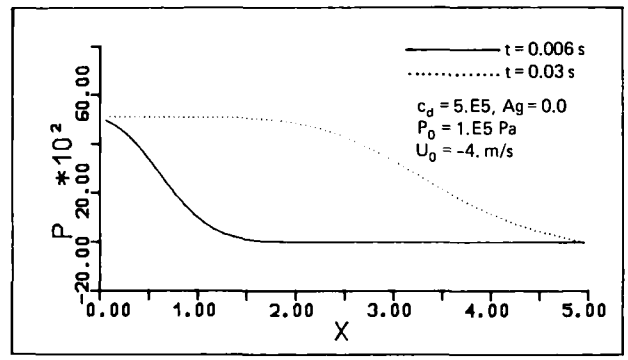

Figure 1 Pressure rise profiles. Air-water system, dispersed flow

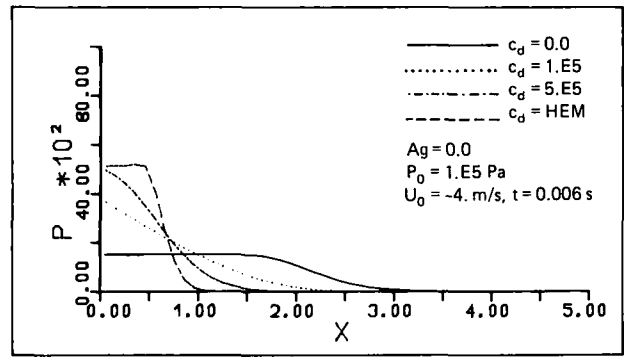

Figure 2 Pressure rise profiles. Air-water system, dispersed flow

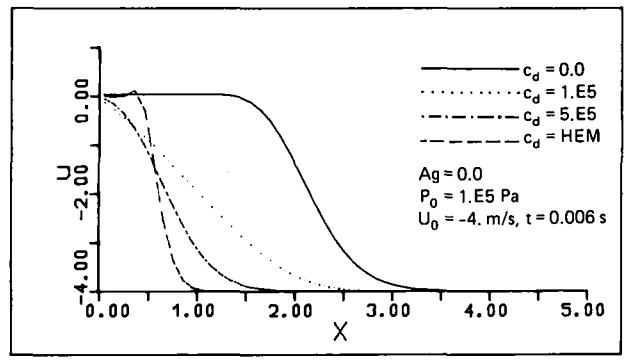

Figure 3 Gas velocity profiles. Air-water system, dispersed flow

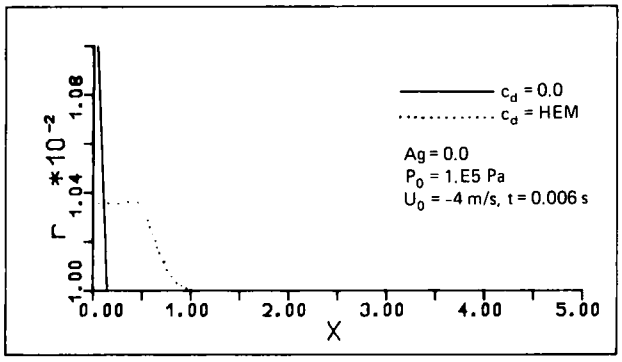

Figure 4 Liquid volume fraction profiles. Air-water system dispersed flow

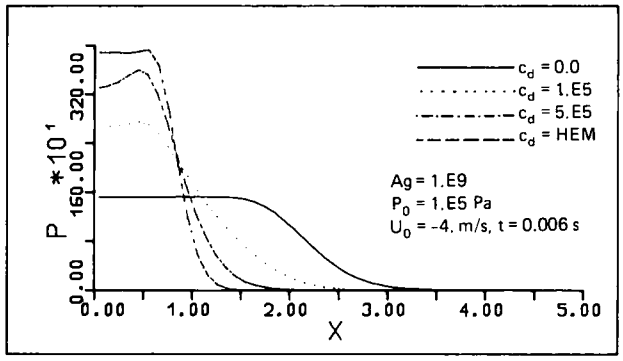

Figure 5 Pressure rise profile. Air-water system, stratified flow

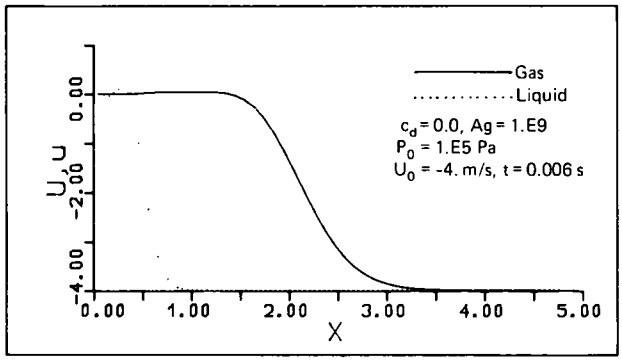

Figure 6 Velocity profiles. Air-water system stratified flow

Stratified flow. When the second pressure is activated, because of the additional link introduced between the two fluids, a number of changes take place. Now, the pressure rise is not high, and the propagation velocities of each flow variable are smaller than the dispersed case (*Figures 5,6*). The most important change, however, is related to the liquid: a gravity wave having been developed with a velocity almost independent of the interphase friction (*Figure 7*) with its height decreasing as the coupling of the liquid with the gas increases.

Steam-water flow with heat and mass transfer

A parametric study was performed for a steam-water flow for different values of the interphase heat transfer coefficients. For simplicity, equal values were assumed for k_{gi} and $k_{\ell i}$. The full set of equations described in the third section was solved.

The developed pressure waves have the same characteristics as those in the isentropic flow discussed previously (*Figure 8*). Wave velocities appear to have increased, but this is justified by the different value of the vapour density. No noticeable change is introduced in the pressure field from the variation in the interphase heat transfer coefficients.

A thermal wave has also formed (*Figure 9*); as the interphase heat transfer coefficient increases, thermal equilibrium tends to be established immediately after the passage of the wavefront (*Figure 9*, $k_g = 1.10^5$).

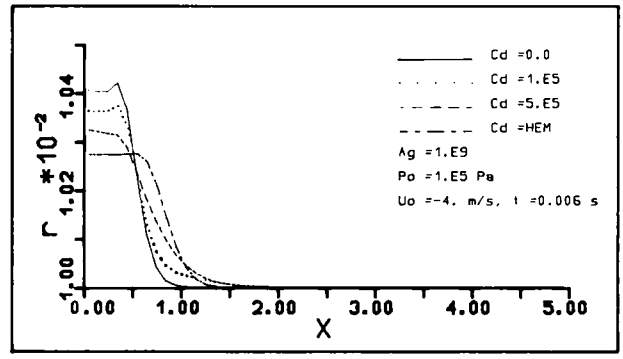

Figure 7 Liquid volume fraction profiles. Air-water system stratified flow

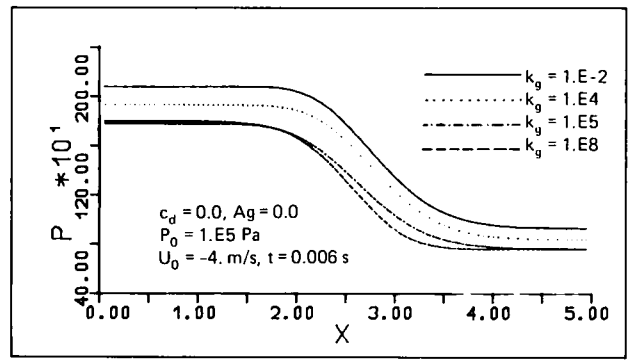

Figure 8 Pressure rise profiles. Steam-water system

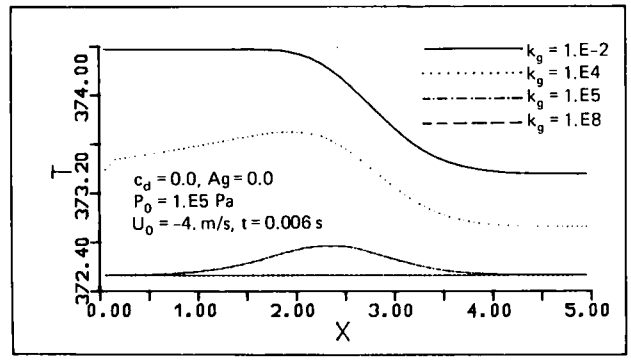

Figure 9 Temperature profiles. Steam-water system

For very large values of this coefficient, complete equilibrium is reached instantaneously and no thermal wave can be detected. The above observations should be related to the corresponding patterns of the mass transfer rate profiles (*Figure 10*). When the interphase transfer coefficient becomes very large, the whole mass transfer process takes place as a "delta"-like pulse following the passage of the thermal wavefront.

Wave velocity

It was mentioned at the beginning that the prediction of wave propagation velocity can be useful in verifying and quantifying nonsteady interactions in two-phase flows. A direct application of this can be realised in the choice of the best time step and grid size. The wave velocity is

$$c = \frac{|\text{the travelling distance of wave}|}{\text{elapsed time}}$$

The travelling distance of the wave was defined as the distance travelled in which the phase velocity reverses direction (zero velocity of the corresponding phase). The computed wave velocities for a frictionless isentropic flow of the air-water system for different grid sizes and time steps are presented in *Figures 11* and *12*. Since the liquid volume fraction is very small, the coupling between the phases is negligible and the predicted wave velocities can be compared to the sonic speed in a single-phase flow given by

$$c = u + \left(\gamma \frac{P_0}{\rho_0}\right)^{1/2}$$

For the grid and time step chosen, the error between predicted and calculated sonic speeds is less than 0.39%.

The calculation of the wave velocities allows the study of the effect that the different parameters have on the flow. In *Figures 13* and *14* the wave velocities are shown for different values of the interphase friction in both dispersed and stratified flows. The existence of a gravity wave for low values of the interphase friction in the stratified flow, as well as the progressive coupling of the two phases with the increase of friction, is illustrated. Pressure and gravity waves degenerate into a single pressure wave when the HEM is activated.

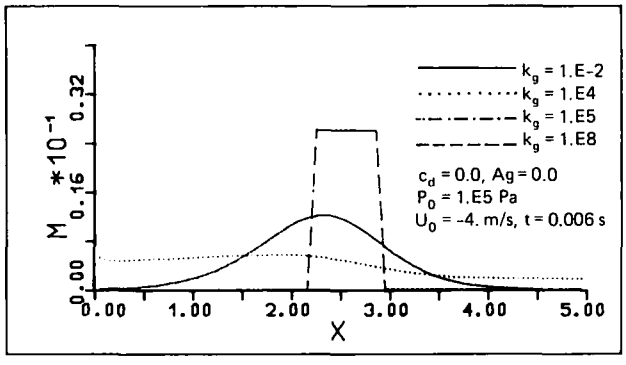

Figure 10 Interphase mass transfer profiles. Steam-water system

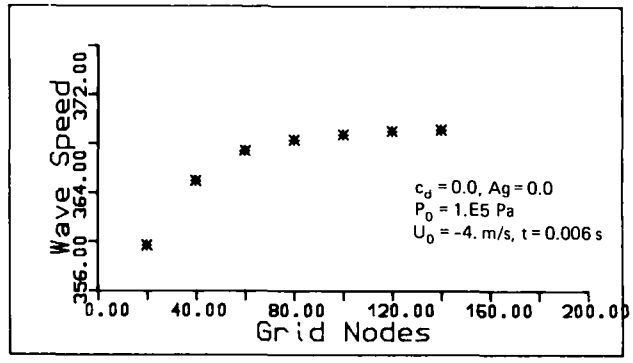

Figure 11 Grid dependence. Air-water system

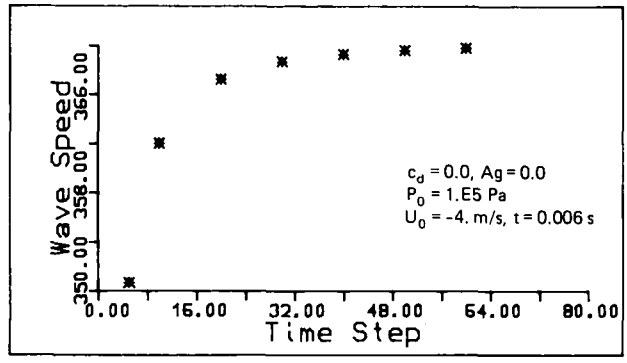

Figure 12 Time dependence. Air-water system

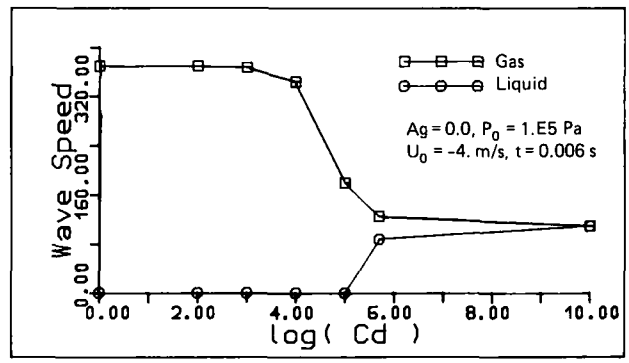

Figure 13 Wave speed versus interphase friction. Air-water system, dispersed flow

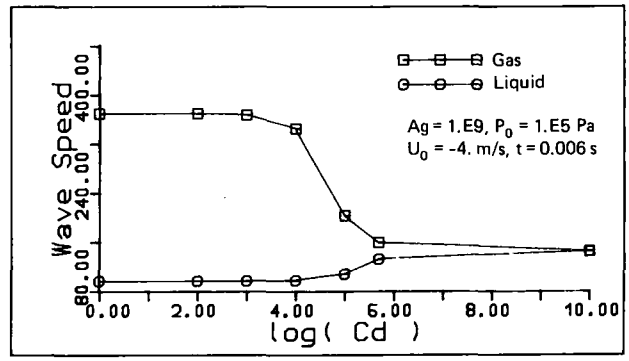

Figure 14 Wave speed versus interphase friction. Air-water system, stratified flow

The predicted value of the wave speed at this limit has a 4% difference from the velocity calculated by the homogeneous model theory.[24]

In *Figure 15* the wave velocities for different values of the liquid volume fraction for a dispersed flow and for two different values of the interphase friction are presented. The characteristic concave shape of the curves as well as the order of magnitude of the wave velocities agrees well with literature data[9,25] in spite of the very simple interphase laws used.

In *Figure 16* the wave velocities for different values of the interphase heat transfer coefficient in the steam-water system are shown. The lower limit of the wave velocity corresponds to thermal equilibrium between the phases; the upper limit is reached when no phase change takes place during the passage of the pressure wave, and it is only determined by the compressibility of the mixture. Comparison with the sonic velocity calculated of an isentropic law (with $\gamma = 1.3$) gives an error of 1.4%.

Comparison with theoretical results

It was pointed out earlier, in the discussion of the air-water system, that when the volume fraction of the liquid is kept low and when the interphase friction is also low the flow conditions are not far from those

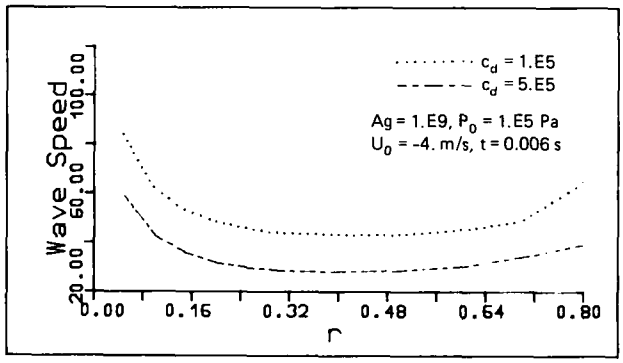

Figure 15 Wave speed versus liquid volume fraction. Air-water system

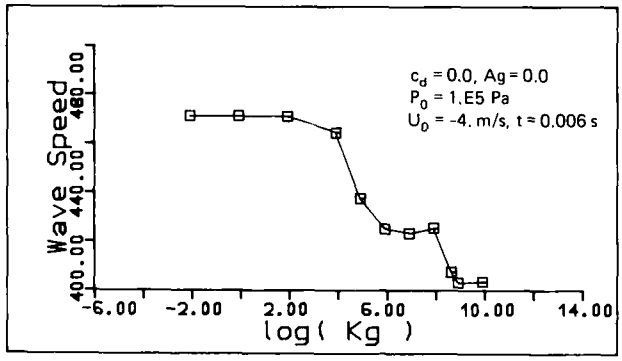

Figure 16 Wave speed versus interphase heat transfer coefficient. Steam-water system

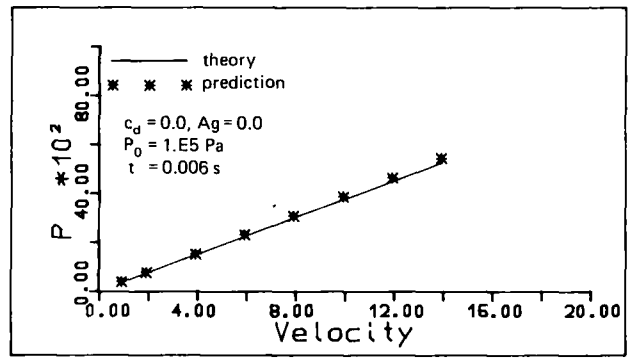

Figure 17 Pressure rise. Air-water system

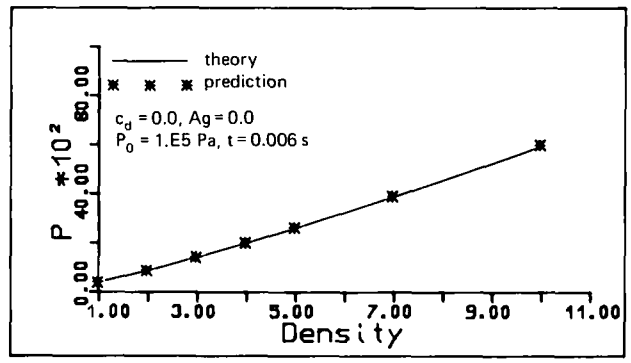

Figure 18 Pressure rise. Air-water system

applying to single-phase flows. This was shown to be the case in the simulation studies in *Figure 14*, where the relative velocity of the pressure and gravity waves gives a measure of the interlinking of the two phases. On the other hand, when the interphase friction is quite large, the coupling of the two fluids is so strong that the results of the homogeneous fluid model theory can be applied. Some simple tests can be devised, then, to check the validity of the model and of the numerical scheme employed at both these limits. The area between limits should be checked against experimental data.

Flow of air-water system with low interphase friction

Gas flow. In a travelling plane wave the initial fluid velocity is related to the pressure rise ΔP and to density in a simple manner:[26]

$$\Delta P = \rho_{g0} c_g u_{g0}$$

where c_g is the sonic velocity. Results from the application of this equation for different values of gas velocity and gas density along with predictions of the present model are shown in *Figures 17* and *18*. Pressure rise follows a linear increase with velocity and density, and in all cases the excellent agreement between theory and simulation is evident.

Flow of liquid. The velocity of the gravity wave and the extent of the rise in the liquid level depend on the initial conditions, and, as can be shown,[1] these two

variables are interrelated by

$$\frac{h_2}{h_1} = 1 + \frac{u_{\ell 0}}{c_\ell} \tag{8}$$

and

$$\left(\frac{h_2}{h_1}\right)^3 - \left(\frac{h_2}{h_1}\right)^2 - (1 + 2\mathrm{Fr})\frac{h_2}{h_1} + 1 = 0 \tag{9}$$

where c_ℓ is the velocity of the gravity wave, h_1 and h_2 are the initial and final heights of the liquid, and Fr is the Froude number, defined by

$$\mathrm{Fr} = \frac{u_{\ell 0}^2}{g h_1}$$

The system (8)–(9) has three real roots for all positive values of h_1 and $\mathrm{Fr} < 1$, the positive ones only being relevant to the present situation. Comparison for different values of the Fr number in *Figure 19* shows the excellent agreement between the predicted and theoretically calculated wave thicknesses.

Flow of air-water system with high interphase friction

It can be shown[24] that the wave velocity of the homogeneous model in such a flow is

$$c^2 = \left[(r_g\rho_g + r_\ell\rho_\ell)\left(\frac{r_\ell}{\rho_\ell c_\ell^2} + \frac{r_g}{\rho_g c_g^2}\right)\right]^{-1}$$

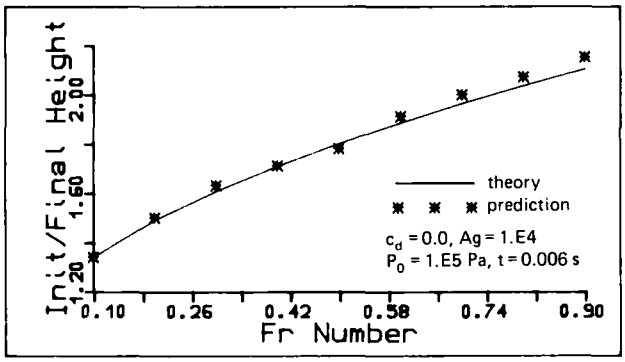

Figure 19 Wave thickness versus Froude number. Air-water system

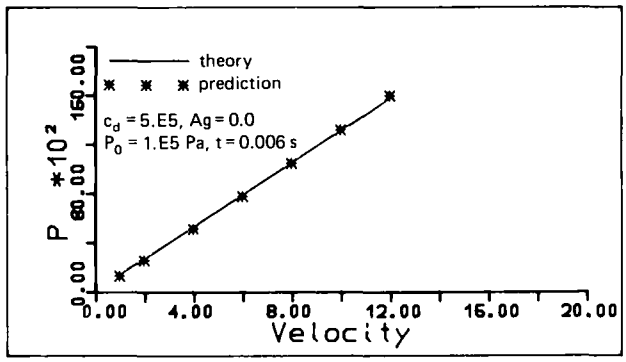

Figure 20 Pressure rise. High friction case. Air-water system

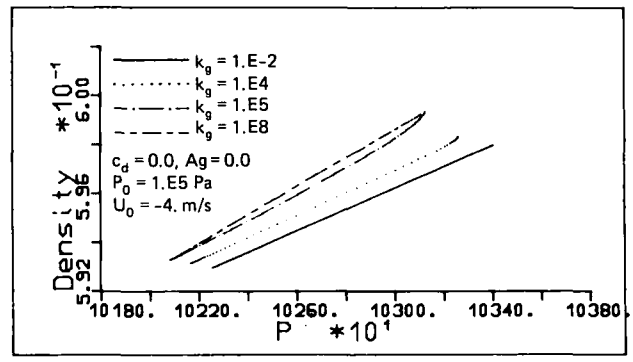

Figure 21 Density-pressure relationship. Steam-water system

When $c_\ell \gg c_g$ and $\rho_\ell > \rho_g$, this is simplified to

$$c = [c_g^2\rho_g/\rho_\ell r_g r_\ell]^{1/2}$$

The calculated and predicted wave velocities are shown in *Figure 20*. Again, complete agreement is found between predictions and theory.

Flow with heat and mass transfer

As we did for the air-water system, we could have specified a priori the nature of the evolution of the stream-water flow relating the pressure to density through an isentropic law. There are two reasons why in this case this practice was not followed. First, the exact nature of the thermodynamic evolution in two-phase flows, because of the different nonequilibrium processes that take place, is not known.[6] Second, we wanted to show that implementation of the transfer laws themselves onto the model can lead to some interesting results. The relation of interphase heat transfer coefficients to wave speed has already been discussed in the last section. Here, their relation to the polytropic exponent (in a generalised isentropic law) will be shown.

Since, initially, the fluid state along the duct was assumed to be uniform, its final states along the duct should lie on the same adiabatic. This curve, then, should represent the polytropic law

$$\rho_g = \alpha P^{1/n} \tag{10}$$

that the evolution of the compressible vapour has followed. In *Figure 21* the pressure field along the duct is plotted against the density field for different values of the interphase heat transfer coefficient. A curve fitting of these state conditions to equation (10) gave a value to the polytropic exponent equal to 1.33 when $k_g = 1.10^{-2}$ (no heat and mass transfer) varying continuously up to 1.0 when k_g tends to infinity.

Conclusions

Simulation of a compressible transient two-phase flow in a duct was carried out. Two different flow regimes and nonequilibrium interphase processes were assumed. Wave propagation was studied, and quantification of different phenomena accompanying the pres-

sure and gravity waves was performed. Numerical results referring to wave velocities, wave pressure rises, wave thickness, and thermodynamic evolution of the compressible phase were compared with available analytical solutions. Verification of the model and the numerical scheme employed in two limiting cases, those of low and high interphase friction was carried out and found to be excellent.

Additional study in this area should concentrate on implementation of more realistic correlations for the interphase processes, the study of other flow regimes, and the adjustment of the model parameters to the available experimental data.

Acknowledgment

The author wishes to express his gratitude to Professor D. B. Spalding for his very constructive criticism and valuable help during the completion of this work.

References

1 Streeter, V. L. and Wylie, E. B. *Hydraulic Transients*. McGraw-Hill, New York, 1969

2 Wijngaarden van L. Waves in gas-liquid flows. In *Theory of Dispersed Multiphase Flow*, ed. R. E. Meyer. Academic Press, New York, 1983, pp. 251–269

3 Mishima, K. and Ishii, M. Theoretical prediction of onset of horizontal slug flow. *ASME J. Fluids Engineering* 1980, **102**, 441–445

4 Andreussi, P., Asali, J. C., and Hanratty, T. J. Initiation of roll waves in gas-liquid flows. *AICHE J.* 1985, **31**, 119–126

5 Moody, F. J. A pressure pulse model for two-phase critical flow and sonic velocity. *ASME Heat Transfer*, August 1969, 371–384

6 Bouré, J. A., Fritte, A. A., Giot, M. M., and Réocreux, M. L. Highlights of two-phase critical flow: on the links between maximum flow rates, sonic velocities, propagation and transfer phenomena in single and two-phase flows. *Int. J. Multiphase Flow* 1976, **3**, 1–22

7 Fischer, M. The dynamics of waves including shocks in two-phase flow. *Nuclear Engrg. Des.* 1969, **11**, 103–131

8 Borisov, A. A., Gelfand, B. E., and Timofeev, E. I. Shock waves in liquids containing gas bubbles. *Int. J. Multiphase Flow* 1983, **9**, 531–543

9 Mecredy, R. C. and Hamilton, L. J. The effects of nonequilibrium heat, mass and momentum transfer on two-phase sound speed. *Int. J. Heat Transfer* 1972, **15**, 61–72

10 Ardron, K. H. and Duffey, R. B. Acoustic wave propagation in a flowing liquid-vapour mixture. *Int. J. Multiphase Flow* 1978, **4**, 302–322

11 Cheng, L. Y., and Drew, D. A., and Lahey, R. T. An analysis of wave propagation in bubbly two-component, two-phase flow. *ASME J. Heat Transfer* 1985, **107**, 402–408

12 Stuhmiller, J. H. The influence of interfacial pressure, forces on the character of two-phase flow model equations. *Int. J. Multiphase Flow* 1977, **3**, 551–560

13 Ardron, K. H. One-dimensional two-fluid equations for horizontal stratified two-phase flow. *Int. J. Multiphase Flow* 1980, **6**, 295–304

14 Wallis, G. B. and Hutchings, B. J. Compressibility effects on waves in stratified two-phase flow. *Int. J. Multiphase Flow* 1983, **9**, 325–336

15 Jones, A. V. and Prosperetti, A. On the suitability of first order differential models for two-phase flow prediction. *Int. J. Multiphase Flow* 1985, **11**, 133–148

16 Spalding, D. B. The calculation of free-convection phenomena in gas-liquid mixtures. In *Turbulent Buoyant Convection*, eds. N. Afgan and D. B. Spalding. Hemisphere, Washington, D.C., 1977, pp. 569–586

17 Baghdadi, A. H. A., Rosten, H. I., Singhal, A. K., Tatchell, D. G., and Spalding, D. B. Finite-difference predictions of waves in stratified gas-liquid flows. In *Two-Phase Momentum, Heat and Mass Transfer*, eds. Durst, Tsiklauri, Afgan. Hemisphere, Washington, D.C., 1979, pp. 471–483

18 Kurosaki, Y. and Spalding, D. B. One-dimensional unsteady two-phase flows with interphase slip: a numerical study. *Second Multi-Phase Flow and Heat Transfer Symposium-Workshop*. Miami Beach, April 1979

19 Spalding, D. B. *IPSA 1981: New Developments and Computed Results*. IMACS Conference, Lehigh University, October 1981

20 Hancox, W. T., Ferch, R. L., Liu, W. S., and Nieman, R. E. One-dimensional models for transient gas-liquid flows in ducts. *Int. J. Multiphase Flow* 1980, **6**, 25–40

21 Stewart, H. B. and Wandroff, B. Two-phase flow: models and methods. *J. Comput. Phys.* 1984, **56**, 363–409

22 Spalding D. B. *Mathematical Methods in Nuclear Reactor Thermal Hydraulics*. American Nuclear Society, Meeting on Nuclear-Reactor Thermal Hydraulics, Saratoga, N.Y., 1980

23 Spalding, D. B. A general purpose computer program for multidimensional one and two-phase flows. IMACS Conference, Legigh, *Mathematics and Computers in Simulation*, Vol. XIII. 1981, pp. 267–276

24 Wallis, G. B. *One-Dimensional Two-Phase Flow*. McGraw-Hill, New York, 1969

25 Grolmes, M. A. and Fauske, H. K. Propagation characteristics of compression and rarefaction pressure pulses in one-component vapor-liquid mixtures. *Nuclear Engrg. Des.* 1969, **11**, 137–142

26 Landau, L. D. and Lifshitz, E. M. *Fluid Mechanics*. Pergamon Press, London, 1959, p. 247